Proceedings of HT2007
2007 ASME-JSME Thermal Engineering Summer Heat Transfer Conference
Vancouver, British Columbia, CANADA, July 8-12, 2007

DRAFT **HT2007-32819**

SPRAY AND COOLING DYNAMICS OF CRYOGEN SPRAYS IMPINGING ON A HUMAN SKIN MODEL

Walfre Franco[1,2]*, Henry Vu[2], Wangcun Jia[1], J. Stuart Nelson[1] and Guillermo Aguilar[2]
[1]Beckman Laser Institute, University of California, Irvine, CA 92612
[2]Department of Mechanical Engineering, University of California, Riverside, CA 92521

ABSTRACT

The objective of the present work is to correlate the time-dependent flow characteristics of cryogen sprays to the induced thermal dynamics at the surface of a human skin model. First, a numerical analysis to evaluate our skin model is carried out. Next, diameter and axial velocity of droplets impinging onto the skin model are measured. Diameter, velocity and surface temperature are acquired simultaneously at the center of the spray cone close to and at the skin model surface, respectively. Spurt durations of 10, 30 and 50 ms are investigated. Finally, measurements are used to compute spray number, mass and kinetic energy fluxes and surface heat flux.

Numerical modeling shows that, subject to the same heat flux, the thermal response of our model and human skin is qualitatively similar but the total temperature drop in skin is about 50% less than that of the model. A simple transformation can be used to map the temperature response of the model to that of skin. Experimental measurements show that during the initial spray transient, fast and small droplets (respect to steady state values) induce large temperature drops and the highest heat flux because the temperature difference between liquid and substrate is the largest; during the spray steady state, surface temperature remains at its lowest value; during the final transient, droplets are fast and small again, although their impact on the surface heat transfer is negligible due to decreasing mass and kinetic energy fluxes and reduced temperature differences between liquid and substrate.

*Address all correspondence to this author; email: wfranco@uci.edu

INTRODUCTION

Cutaneous laser surgery assisted by cryogen spray cooling has proven essential in cutaneous and cosmetic laser surgery. A short cryogen spurt precools the epidermis to avoid excessive, unintended injury therein during laser irradiation from excessive heating induced by melanin absorption of laser light [1]. Heat extraction from skin during CSC is a function of many fundamental spray parameters, such as average droplet diameter and velocity, mass flow rate, temperature and spray density among others [2], that vary in time and space within the spray cone.

The objectives of the present study are the following: (i) to evaluate an epoxy block substrate as a thermal model of human skin; (ii) to determine the flow characteristics of cryogen sprays in transient state impinging onto the human skin model; (iii) to correlate the spray characteristics to the surface heat transferred from the human skin model.

EXPERIMENTAL AND NUMERICAL METHODS

First, a numerical analysis to evaluate an epoxy block substrate as skin model is carried out. Next, an epoxy substrate with an embedded thin foil sensor is used to measure surface temperatures, and a phase doppler particle analyzer (PDPA) is used to measure the diameter and axial velocity of cryogen droplets impinging onto the skin model with thermal sensor. PDPA and surface temperature measurements are acquired simultaneously at the center of the spray cone 32.5 and 35 mm downstream from the nozzle tip, respectively. Spurt durations of 10, 30 and 50 ms are investigated. Finally, the surface heat flux is computed using the solution of a direct heat conduction problem, and spray num-

Copyright © 2007 by ASME

	epidermis	epoxy
k (W/m K)	0.21	0.14
ρ (kg/m^3)	1200	1019
c (J/kg K)	3600	1631
α (m^2/s)	4.9×10^{-8}	8.4×10^{-8}

Table 1. Thermal properties of epidermis [6] and epoxy [7].

ber, mass and kinetic energy fluxes are computed using Roisman and Tropea's algorithm [3].

Spray System

Refrigerant hydrofluorocarbon 134a (Suva ®134a, Dupont) is delivered through a high pressure hose to an electronic valve (Series 99, Parker Hannifin Corp., Cleveland OH) attached to an angled-tube nozzle with 40 mm length and ≈ 0.5 mm inner diameter; valve and nozzle are part of a commercial skin cooling device (GentleLase, Candela, Wayland MA). The valve is set to deliver a downward vertical spray in our experimental set up. R134a has a boiling temperature at atmospheric pressure of ≈ -26 °C and is kept in its original container at a pressure of 600 kPa and room temperature of 21 °C. In this study, we will look into 10, 30 and 50 ms spurts delivered 35 mm away nozzle-skin distance.

Thermal Sensor and Human Skin Model

A thin-foil K type thermocouple (CO2-K, Omega Engineering, Stamford CT) is used to measure surface temperatures on a human skin model. Although the width and length of its measurement junction are ≈ 0.5 mm, the thin-foil sensor has a thickness of 13 μm that provides high vertical temperature resolution. This feature makes the sensor suitable for measuring surface temperature during CSC because the vertical temperature gradient in either skin phantom or human skin is much larger than that in the lateral direction [4]. The estimated response time is around 2 ms and measurement uncertainty associated with K-type thermocouples is about 0.28 °C after calibration. The skin model is composed of an epoxy resin (EP30- 3, Master Bond, Inc., Hackensack NJ), which contains the embedded thermal sensor at the surface level. Thermal properties of epidermis and epoxy are shown in Table 1 and details about preparation of the skin model can be found in [5]. The sensor is placed at the center of the spray cone, where the highest heat extraction occurs. The human skin model is referred as skin phantom herein.

Heat Flux Calculations

Temperatures recorded by the thin-foil sensor are assumed to be surface temperatures because the foil Biot number (hL/k) for a heat transfer coefficient $h = 20,000$ W/(m^2·K) [8], characteristic length $L = 13\times10^{-6}$ m and thermal conductivity $k = 12$ W/(m·K) [9] is $\approx 2\times10^{-2}$; i.e., the temperature of the foil is spatially uniform, $hL/k << 1$. The following analytical expression based on Fourier's law and Duhamel's theorem is used to compute the surface heat flux q from temperature measurements T:

$$q_I = 2\sqrt{\frac{k\rho c}{\pi}}\sum_{i=1}^{I}\frac{T_i - T_{i-1}}{\sqrt{t_I - t_i}+\sqrt{t_I - t_{i-1}}} \tag{1}$$

where I is the total number of measurements, ρ the density, c the specific heat, and t the time. A detailed derivation of Eq. 1 can be found in [4, 10].

Heat Transfer Modeling

To model the thermal response of human skin and epoxy to cryogen spray cooling, we solve the-two dimensional heat conduction equation:

$$\rho c\frac{\partial}{\partial t}T(x,y,t) - \nabla(k\nabla T(x,y,t)) = 0, \tag{2}$$

for which the surface boundary condition is specified as

$$-k\nabla T(x,0,t)\cdot\vec{n} = q(t). \tag{3}$$

x and y are respectively the lateral and vertical coordinates, $\vec{n}$ is the unit vector normal to the surface and q is the surface heat extraction computed from experimental measurements using Eq. 1. At the other boundaries $-k\nabla T\cdot\vec{n} = 0$. The computation domain is the following: -1×10^{-3} m $\le x \le 1\times10^{-3}$ m, -1.5×10^{-3} m $\le y \le 0$ m. Thermal properties of epidermis and epoxy are shown in Table 1.

Phase Doppler Anemometry and Particle Sizing

Spray droplet velocity and diameter are measured with a phase doppler particle analyzer (PDPA; TSI Incorporated, Shoreview MN). This system is capable of measuring velocity along two perpendicular axes, but only axial velocities are considered herein because measurements correspond to the cone center of vertical cryogen sprays; that is, the magnitudes of lateral velocities and data rates are significantly smaller than their axial counterparts. The PDPA measurement volume is set 2.5 mm above the thin-foil surface sensor embedded in the skin model. For the spray transient analysis, velocity and diameter measurements are split in 1 ms time windows. Approximately 10 runs are made for each spurt duration under study to allocate a minimum of 100

Copyright © 2007 by ASME

data points in each time bin. The deviation percentage from the cumulative size distribution as a function of the sample size N can be estimated as $127.32 \cdot N^{-0.492}$ [11], which corresponds to a maximum deviation of 13% in our study.

Spray Flux Calculations

Number, mass and kinetic energy fluxes of cryogen sprays are estimated from PDPA measurements following [3]:

$$\varphi = \frac{1}{\tau} \sum_{i=1}^{N_v} \frac{\eta_i \varphi_i}{A_{\gamma,i}(D_i, \gamma_i)} \vec{e}_{\gamma,i}, \tag{4}$$

where

$$\varphi_i = \begin{cases} 1 & \text{for the number flux,} \\ \frac{\pi\rho}{6} D_i^3 & \text{for the mass flux,} \\ \frac{\pi\rho}{12} D_i^3 V_i^2 & \text{for the kinetic energy flux.} \end{cases} \tag{5}$$

τ is the measurement time, N_v is the number of validated signals, η is a correction factor, A_γ is the reference area of the detection volume, D is the diameter of the ith drop, γ is the particle trajectory angle, $\vec{e}_\gamma$ is the unit vector in the direction of the drop motion, ρ is the density, and V the drop velocity. η accounts for count errors due to multiple particles scattering or for non-validation of particles, it is a function of the relative signal presence (in the measured volume) of validated and nonvalidated signals. We use the coincident mode of our PDPA system to define validated signals; within this operational mode, a diameter measurement corresponds to a simultaneous velocity measurement. With the coincident mode off, every signal corresponds to a velocity measurement but not necessarily to a diameter measurement. In addition to D and γ, A_γ is also a function of V, burst duration and hardware parameters (such as the width of the projected slit and the receiver off-axis angle). Details about the computation of η and A_γ are not repeated in this paper. Instead, the reader is referred to [3].

RESULTS AND ANALYSIS

Droplet velocity V and diameter D and surface temperature T are measured simultaneously. Spray system and thermal sensors are placed inside of a chamber in order to maintain a reduced, constant humidity level (16–18%), which otherwise varies significantly during the day and is known to affect the efficiency of the heat extraction from the skin [12,13]. The chamber, described in [14], is made out of transparent acrylic walls that are perpendicular to the PDPA transmitter (laser beams) and receiver (photodetectors).

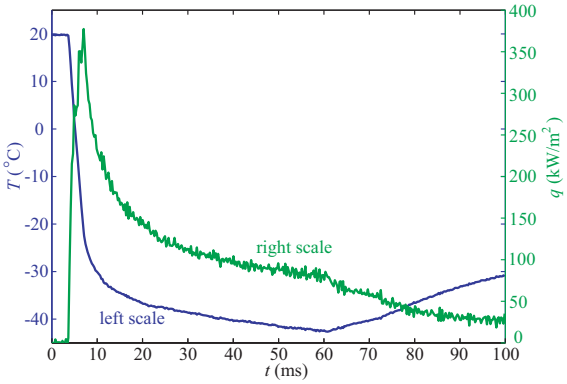

(a) Experiments on epoxy phantom

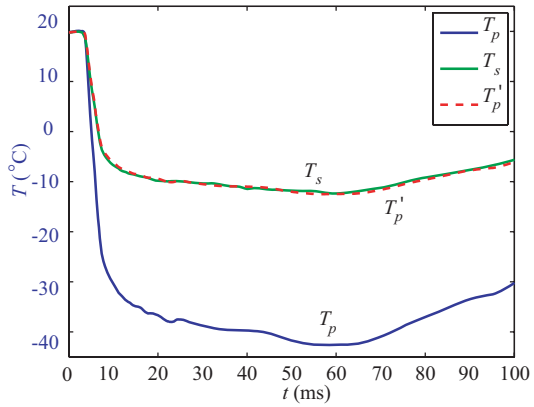

(b) Modeling of phantom and human skin response

Figure 1. (a) Experimental surface temperature (left scale) and estimated surface heat flux q (right scale). (b) Skin and phantom temperature response, T_s and T_p, to q, and mapped temperature T_p' matching skin response.

An Epoxy Substrate as a Human Skin Phantom

Figure 1(a) shows the experimental surface temperature T_e (left scale) during CSC of the skin phantom with a 50 ms spurt. The corresponding surface heat flux q (right scale) is shown in the same figure. This heat flux is next used as the boundary condition for comparing the thermal response between human skin and skin phantom. Figure 1(b) shows numerical surface temperatures of the skin T_s and phantom T_p . The largest temperature drops in skin and phantom (ΔT_s and ΔT_p) are 32 and 66 °C, respectively; temperature drops are 92% and 86% of ΔT_s and ΔT_p, respectively, at $t = 20$ ms; lowest surface temperatures, -12.4 and -46.2 °C, occur at $t \approx 59$ and 57 ms, respectively. Although the dynamic responses of phantom and skin to the same time-dependent heat flux are qualitatively similar, T_p is significantly lower than T_s. This is not surprising at all since the density—and mass for the same volume—and ability to conduct thermal energy of these materials are comparable; however, more heat

Copyright © 2007 by ASME

is needed to change the temperature of the skin than that of the epoxy, Table 1.

It is possible to introduce a simple transformation to map T_p to T_s as follows:

$$T_p'(t) = T_o + \xi(T_p(t) - T_o), \tag{6}$$

where T_o is the initial temperature of the phantom and

$$\xi = \frac{k_p\sqrt{\alpha_s}}{k_s\sqrt{\alpha_p}}. \tag{7}$$

The transformation is based on the analytical solution for constant surface heat flux evaluated at the surface [9]. Mapping of the epoxy surface temperature response to that of skin, T_p', is shown in Fig. 1(b), $T_p' = T_s$.

Our results show that assuming that the heat transferred from an epoxy skin phantom during CSC is the same as that from skin, ΔT_s is approximately 50% of ΔT_p. But the problem is far more complex, q is a function of the substrate thermal properties and the spray thermodynamics, such as, phase (liquid, vapor) and temperatures among others. Dynamics of q during CSC of human skin may be similar to those reported in this study; however, q might be quantitative smaller and, subsequently, T_s may drop even less than what is shown in Fig. 1(b).

Fluid and Heat Transfer Dynamics during CSC

Spray Fluid Dynamics. The count of coincident and noncoincident measurements in each 1 ms bin for 10, 30 and 50 ms spurts is shown in Fig. 2. Except for the last two bins in each figure (which are excluded from computations), there are more than 100 samples per bin. The difference between noncoincident and coincident measurements counts represents the number of nonvalidated particle size measurements, which in our PDPA system correspond to mismatches between two independent phase shift (particle size) measurements; hence, there is only a velocity measurement. This situation may arise, for example, when there are two or more drops in the probe volume simultaneously.

Droplet mean velocity V and diameter D as a function of time during 10, 30 and 50 ms spurts are shown in Fig. 3. The times at which steady states begin, $\overline{t_o}$, and end, $\overline{t_f}$, are represented by vertical dashed lines. Cryogen droplets take ≈ 4 ms to reach the skin phantom surface from the time at which the valve is energized. Independent measurements of laser light transmittance at the nozzle exit (not included) show that this initial delay is mainly due to the valve's opening mechanics. Furthermore, if the initial droplets $V > 50$ ms, their in-flight time from the nozzle to the phantom surface is < 0.07 ms which is only a small fraction

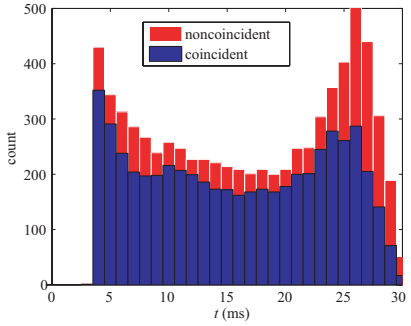

(a) 10 ms spurt

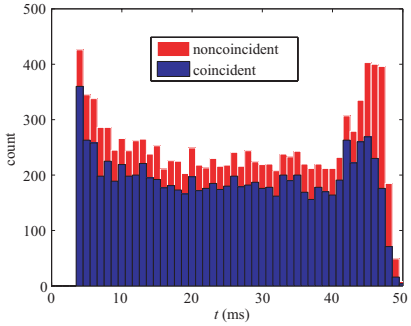

(b) 30 ms spurt

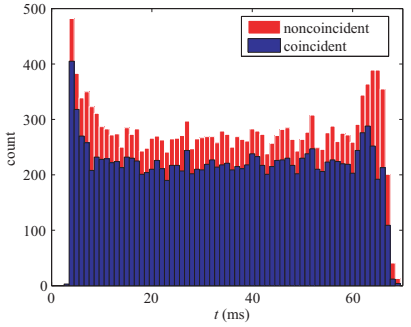

(c) 50 ms spurt

Figure 2. Count of coincident and noncoincident measurements in 1 ms time bins during spurt duration.

of the total delay. For each spurt, the initial and final spray transients respectively last ≈ 4 and 10 ms; these are the times that the valve takes to fully open and close, respectively. Figure 3(a) shows that during the initial transient, $t = 4$–8 ms, V increases reaching a maximum of 55 m/s, then decreases to reach steady state value $\overline{V} = 48$ m/s. During the final transient, V increases monotonically beyond its initial transient maximum value. Final transients begin 8 ms after the period in which the valve is energized (i.e., nominal spurt duration) ends—these times are also the end of the steady state, vertical dashed lines $\overline{t_f}$ in the figures.

Copyright © 2007 by ASME

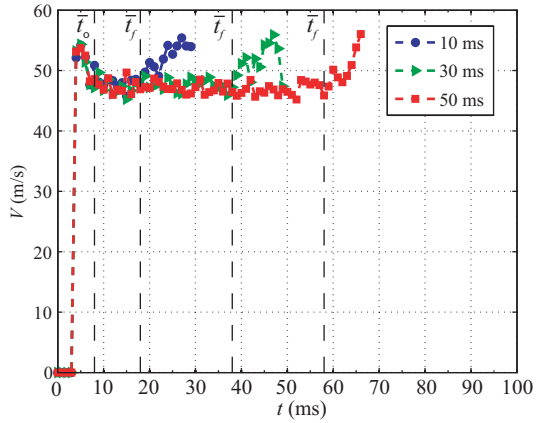

(a) Dynamics of droplet velocity

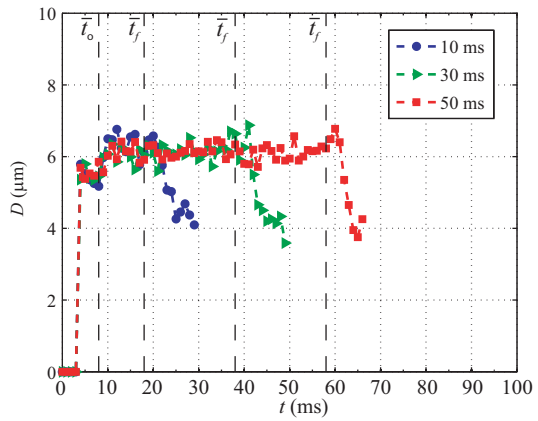

(b) Dynamics of droplet diameter

Figure 3. Cryogen droplet mean velocity and diameter as a function of time during 10, 30 and 50 ms cryogen spurts. Vertical dashed lines represent the beginning and end, $\overline{t}_o$ and $\overline{t}_f$, of the spray steady state.

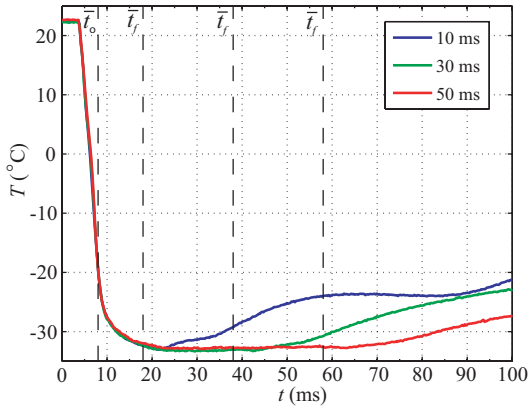

(a) Dynamics of surface temperature

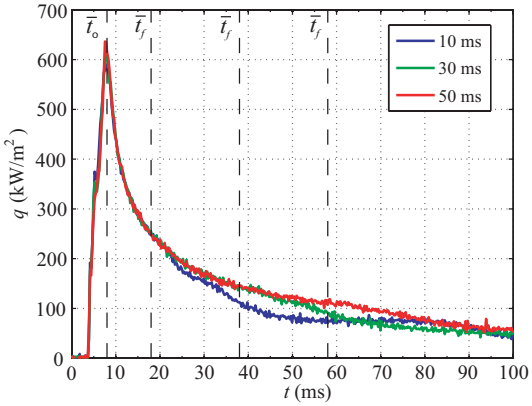

(b) Dynamics of surface heat flux

Figure 4. Skin phantom mean surface temperature and heat flux as a function of time during 10, 30 and 50 ms spurts. Vertical dashed lines represent the beginning and end, $\overline{t}_o$ and $\overline{t}_f$, of the spray steady state.

Figure 3(b) shows that during the transient states, D decreases and increases when V increases and decreases, respectively; that is, small droplets travel faster than larger droplets and vice versa. $\overline{D} = 6$ μm.

Surface Heat Transfer Dynamics. The skin phantom mean surface temperature T and heat flux q as a function of time during 10, 30 and 50 ms spurts are shown in Fig. 4. Vertical dashed lines represent the spray $\overline{t}_o$ and $\overline{t}_f$, which are included to facilitate the transient-state correlation between spray characteristics and phantom cooling. As in the spray fluid dynamics, initial and final temperature transients can be identified in Fig. 4(a): initially, T decreases abruptly during the first 6 ms ($t = 4$–10 ms), continues decreasing at a lower rate during the next 10 ms ($t = 10$–20 ms), and, finally, reaches steady state $\overline{T} = -33$ °C, which is also the lowest surface temperature T_l; during the final transient, T slowly increases to reach room temperature. Figure 4(b) shows that q is highly dynamic: q increases abruptly reaching a maximum 5 ms after the droplets arrive to the surface; subsequently, q decreases at different rates from high to low—as evidenced by slope changes in the curves. The highest heat flux $q_h = 591$ ($t = 8.1$ ms), 611 (7.8 ms) and 636 kW/m^2 (7.5 ms) for 10, 30 and 50 ms spurt durations, respectively. Figures 4(a) and (b) also show that increasing the spurt duration, increases the time for which the surface remains at T_l (or $\overline{T}$), and decreases the rate of change of q that increases T back to room temperature. This in agreement with previously reported results in [15, 16], except that T_l was reported to depend on the spurt duration. In the present study $T_l = -33$ °C for each spurt duration, Fig. 4(a). This discrepancy may be due to differences in thermal sensors, spray system and experimental conditions (such as humidity levels) between the cited and present study.

Copyright © 2007 by ASME

Spray and Skin Phantom Fluid-Thermal Interactions

It is during the initial spray transient when small and fast droplets wet the phantom surface and the largest temperature drops and highest heat flux occur because the temperature difference between the cryogenic liquid and warm substrate is the largest. If T is lower than the boiling temperature of cryogen T_b, it is reasonable to assume that there is liquid cryogen on the surface. It follows that during most of the spray steady state the surface is wet with a pool of liquid since $T < T_b$. For the 30 and 50 ms spurts, once there are no more incoming droplets T departs from $\overline{T}$ ($t \approx 50$ and 65 ms). For the 10 ms spurt, this departure occurs during the spray final transient state; a shorter spray duration implies less accumulation of liquid cryogen during the spray steady state, and, consequently, a surface—with a thinner pool—more sensitive to small changes.

During the final transient, droplets are smaller and faster but do not enhance the surface heat transfer at all. During this transient, there is an increase in the number flux followed by a decrease, Fig. 5 (a)–(c), while the mass flux, Figs. 5 (d)–(f), and kinetic energy flux, Figs. 5 (g)–(i), only decrease. Therefore, during the final transient, droplets have less energy to pierce or stir the liquid pool enhancing the heat transfer, and may end up accumulating on top, which is not significant either due to low mass flux. Furthermore, even if these droplets impinged on a surface free of cryogen, the temperature difference between liquid and substrate would be small resulting in small heat fluxes.

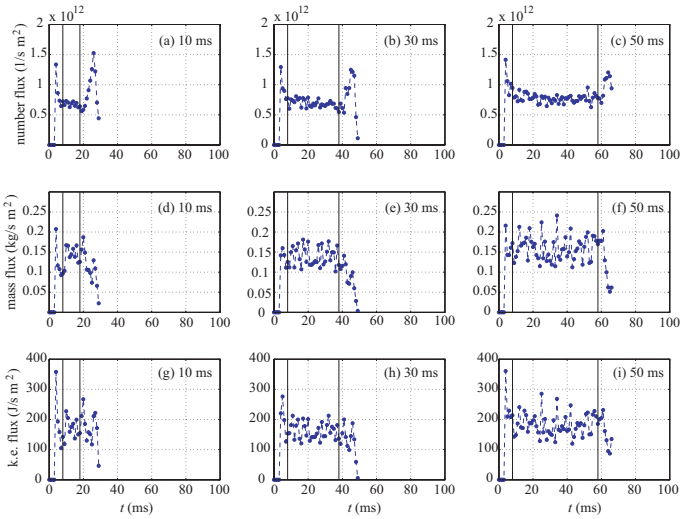

Figure 5. Spray number, (a)–(c), mass, (d)–(f), and kinetic energy, (g)–(i), flux during 10, 30 and 50 ms spurts. Vertical dashed lines represent the beginning and end (left and right line, respectively) of the spray steady state.

CONCLUSIONS

Numerical modeling of epoxy and human skin show that, subject to the same heat flux, their thermal response is qualitatively similar but the total temperature drop in skin is about 50% less than in the epoxy. A simple transformation can be used to map the temperature response of the epoxy to that of skin. Experimental measurements of droplet velocity and diameter and skin phantom surface temperature, show that during the initial spray transient, fast and small droplets (respect to steady state values) induce large temperature drops and the highest heat flux since the temperature difference between cryogen and skin phantom is the largest; during the spray steady state, surface temperature remains at its lowest value; during the final transient, droplets are fast and small again, although in this period their impact on the surface heat transfer is negligible due to decreasing mass and kinetic energy fluxes and, especially, reduced temperature differences between cryogen and skin phantom.

ACKNOWLEDGMENT

This work was supported by the following grants: AR47551, AR48458 and GM62177 to JSN and HD42057 to GA from the National Institutes of Health.

REFERENCES

[1] Nelson, J., Milner, T., Anvari, B., Tanenbaum, B., Kimel, S., Svaasand, L., and Jacques, S., 1995. "Dynamic epidermal cooling during pulsed-laser treatment of port-wine stain - a new methodology with preliminary clinical evaluation". *Arch Dermatol*, **131**(6), pp. 695–700.

[2] Aguilar, G., Majaron, B., Pope, K., Svaasand, L. O., Lavernia, E. J., and Nelson, J. S., 2001. "Influence of nozzle-to-skin distance in cryogen spray cooling for dermatologic laser surgery". *Lasers Surg. Med.*, **28**(2), pp. 113–120.

[3] Roisman, I. V., and Tropea, C., 2001. "Flux measurements in sprays using phase doppler techniques". *Atomiz. Sprays*, **11**(6), Nov-Dec, pp. 667–699.

[4] Franco, W., Liu, J., Wang, G. X., Nelson, J. S., and Aguilar, G., 2005. "Radial and temporal variations in surface heat transfer during cryogen spray cooling". *Phys. Med. Biol.*, **50**(2), Jan, pp. 387–397.

[5] Jia, W., Aguilar, G., and Nelson, J. S., 2006. "Improvement of port wine stain laser therapy through multiple-intermittent cryogen spurts and two-wavelength laser pulses". *Lasers Surg. Med.*, pp. 3–3.

[6] Duck, F., 1990. *Physical properties of tissue.* Academic press, London.

[7] Tunnell, J. W., Torres, J. H., and Anvari, B., 2002. "Methodology for estimation of time-dependent surface heat flux due to cryogen spray cooling". *Ann. Biomed. Eng.*, **30**(1), Jan, pp. 19–33.

[8] Jia, W., Aguilar, G., Wang, G. X., and Nelson, J. S., 2004. "Heat-transfer dynamics during cryogen spray cooling of

Copyright © 2007 by ASME

substrate at different initial temperatures". *Phys. Med. Biol.*, **49**(23), Dec, pp. 5295–5308.

[9] Incropera, F., and Dewitt, D., 1996. *Fundamentals of heat and mass transfer*. Wiley, New York.

[10] Beck, J., Blackwell, B., and St. Clair, Jr., C., 1985. *Inverse heat conduction: ill posed problems*. Wiley, New York.

[11] Tate, R., 1982. "Some problems associated with the accurate representation of droplet size distributions". In Proceeddings of the 2nd ICLASS.

[12] Majaron, B., Kimel, S., Verkryusse, W., Aguilar, G., Pope, K., Svaasand, L., Lavernia, E., and Nelson, J., 2001. "Cryogen spray cooling in laser dermatology: effects of ambient humidity and frost formation". *Lasers Sur. Med*, **28**(5), pp. 469–476.

[13] Franco, W., Liu, J., and Aguilar, G., 2005. "Interaction of cryogen spray with human skin under vacuum pressures". In Fluid Structure Interaction and Moving Boundary Problems, C. S, H. S, and B. CA, eds., Vol. 84, Wessex Institute of Technology, pp. 153–162.

[14] Vu, H., Franco, W., Jia, W., and Aguilar, G., 2006. "Effects of ambient pressure on r134a sprays for laser dermatological applications". In 19th Annula ILASS Conference.

[15] Aguilar, G., Wang, G. X., and Nelson, J. S., 2003. "Dynamic behavior of cryogen spray cooling: Effects of spurt duration and spray distance". *Lasers Surg. Med.*, **32**(2), pp. 152–159.

[16] Aguilar, G., Wang, G., and Nelson, J., 2003. "Effect of spurt duration on the heat transfer dynamics during cryogen spray cooling". *Phys. Med. Biol.*, **48**(14), pp. 2169–2181.

Copyright © 2007 by ASME